

Theoretical study of rate coefficients and branching fractions in the propene + OH reaction

Judit Zádor*, Ahren W. Jasper, James A. Miller

Combustion Research Facility, MS 9055, Sandia National Laboratories, Livermore, CA 94551-0969 USA

Abstract

High-level *ab initio* calculation of the $C_3H_6 + OH$ potential energy surface was coupled with master equation methods to compute rate coefficients and product branching ratios for temperatures of 300–2500 K. Our model reproduces the available experimental results well. We find a surprisingly wide range of bimolecular product channels for this reaction, including vinyl alcohol, acetaldehyde, allyl radical, acetone, ethene, propanal, propenol and formaldehyde.

Introduction

Alkenes comprise a substantial fraction of practical fuels. The chemistry of propene combustion is of particular interest because it can serve as a prototype for alkene chemistry and because it is simple enough to be thoroughly analyzed. Propene combustion readily leads to the formation of allyl radicals, one of the resonance-stabilized radicals that contribute to soot formation in flames. Experimentally, propene combustion is studied in flames (e.g. Ref. 3), and detailed kinetic mechanisms also exist in the literature (e.g. Refs. 4-6).

The overall rate coefficient of the title reaction has been extensively studied experimentally (e.g. Refs. 7-11) and is reported in data evaluations^{1, 2} for a wide temperature range. The addition of the OH radical to the double bond is dominant below ~500 K and has a negative temperature dependence. Above ~700 K abstraction is the principal process, and the temperature dependence is positive. There is only one study on the bimolecular product distribution at low pressures.¹² The reaction is also intimately linked to the OH-initiated oxidation of propanol,^{13, 14} and the knowledge of the rate coefficient is important in measurements of hydroxypropene + O_2 rate coefficients.

There have been theoretical calculations for portions of the underlying C_3H_7O potential-energy surface (PES).¹⁵⁻¹⁸ However, there is a lack of accurately calculated detailed rate coefficients and product channels for a wide pressure and temperature range.

In this work we calculate the overall rate coefficient and the branching fractions for the 300–2500 K temperature and zero to infinite pressure ranges using high-level *ab initio* methods and RRKM-based multiwell master equation methods. Due to the limitations of paper length, only selected results are presented here.

Construction of the PES

Optimized geometries, frequencies, internal rotational potentials, and energies of the stable

complexes and saddle points along the intrinsic reaction coordinate (IRC) were calculated on the C_3H_7O potential energy surface. Geometry optimization and IRC scans were performed with density functional theory (DFT) calculations using the B3LYP functional applying the d,p-polarized split valence 6-311++G(d,p) Gaussian basis set. In all cases lowest energy conformers were searched for in a systematic manner. For the computation of accurate single point energies we used the restricted quadratic-configuration-interaction method with single and double excitations and correction for triple excitations, RQCISD(T), with the cc-pVnZ basis set, $n = (T, Q)$, extrapolated to the infinite basis set limit cc-pV ∞ Z.¹⁹ The DFT calculations were performed using the Gaussian 03 suite of programs,²⁰ and other quantum chemical calculations employed the MOLPRO package.²¹

Calculation of rate coefficient

RRKM/master-equation (ME) methodology developed by Miller and Klippenstein²²⁻²⁴ was used to determine rate coefficients from the computed stationary point properties. The low-frequency torsional modes were treated as hindered rotors using the Pitzer-Gwinn approach²⁵ applied to state densities. The hindering potentials were determined by fitting Fourier series to the B3LYP/6-311++G(d,p) energies along the internal rotation. Asymmetric Eckart barriers were used to model tunneling in 1D. Collisional energy transfer was approximated by a simple exponential-down model, where the average downward transfer parameter $\langle \Delta E_d \rangle$ was temperature-dependent in the form $200 \times (T/298)^{0.85} \text{ cm}^{-1}$. Lennard-Jones parameters for the C_3H_7O isomers were taken as that of propanol,²⁶ $\sigma = 4.459 \text{ \AA}$, $\epsilon/k_B = 576.7 \text{ K}$. The multiwell ME calculations were carried out with the VARIFLEX program package.²⁷

The entrance channel of the reaction has a van der Waals well corresponding to the OH roughly midway between the two C-atoms of the double bond in

* Corresponding author: jzador@sandia.gov

Proceedings of the European Combustion Meeting 2009

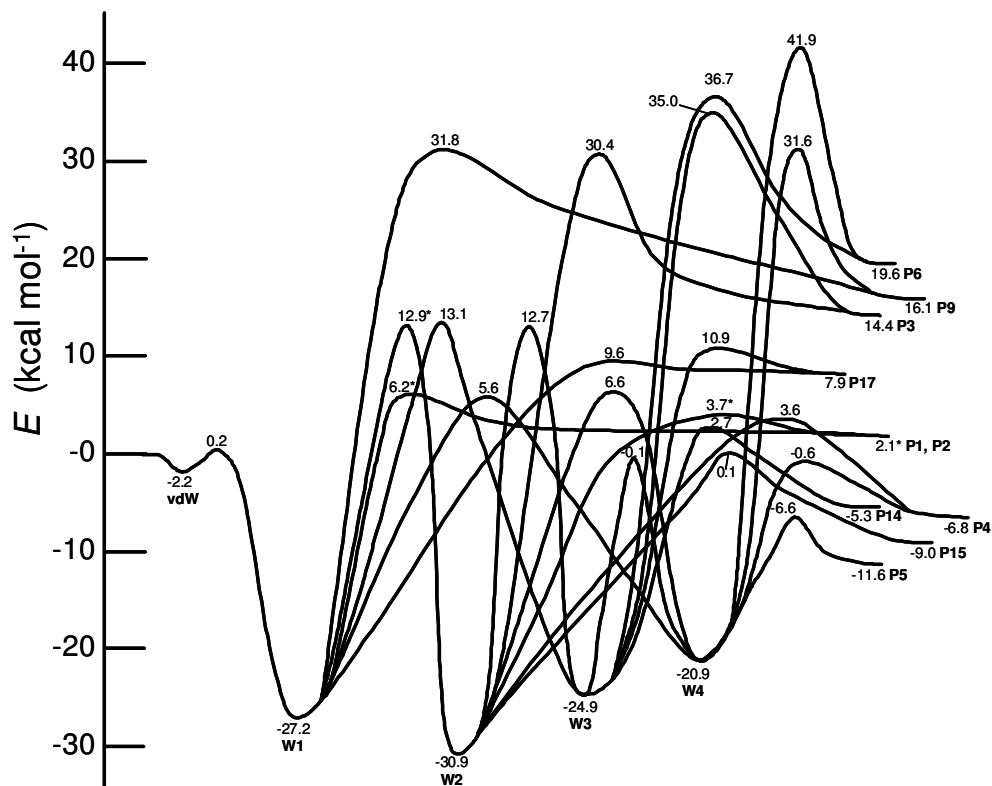


Figure 1. PES for the addition on the terminal carbon atom. The calculated stationary point energies are obtained by RQCISD(T)/cc-pV ∞ Z//B3LYP/6-311++G(d,p) and include the ZPE. The names of the species can be found in Table 1. Starred stationary points have cis-trans isomers, from which only the lower energy one is presented for clarity. The height of the inner transition state $\text{vdW} \leftrightarrow \text{W1}$ is lowered to $-2.3 \text{ kcal mol}^{-1}$ in the rate coefficient calculations (see text).

propene. There is a small barrier for addition to each of the C-atoms. The microcanonical, J -resolved (J is the total angular momentum) number of states for the barrierless entrance to the van der Waals well was calculated variationally using the direct variable-reaction-coordinate transition-state theory (VRC-TST).^{28, 29} The distance between the midpoint of the C-C double bond and the O atom was taken as a reaction coordinate and allowed to change between 4.2 and 10.0 Å. The position of the pivot point on the propene molecule was chosen this way to be able to compare the results better to the $\text{C}_2\text{H}_4 + \text{OH}$ system^{30, 31} with which the propene + OH reaction shows a lot of similarities. The potential energy was evaluated using the CASPT2(5e,4o)/cc-pVDZ method. The effect of geometry relaxation on the computed rates was determined to be negligible as the geometries of the isolated fragments and the van der Waals complex are very close. The VRC-TST calculations were carried out using the VaReCoF code.³²

The overall rate coefficient at very low temperatures is controlled by the long-range dynamical bottle-neck associated with the outer, barrierless transition state, while at higher temperatures it is controlled by the inner transition-states associated with the saddle points for each addition. The effective transition state number of

states for the addition to the terminal and the central carbon atoms, $N_{1,\text{eff}}^\ddagger(E, J)$ and $N_{2,\text{eff}}^\ddagger(E, J)$, respectively, are given by the following equations:

$$N_{1,\text{eff}}^\ddagger(E, J) = \frac{N_{\text{outer}}^\ddagger(E, J) \times N_1^\ddagger(E, J)}{N_{\text{outer}}^\ddagger(E, J) + N_1^\ddagger(E, J) + N_2^\ddagger(E, J)}$$

and

$$N_{2,\text{eff}}^\ddagger(E, J) = \frac{N_{\text{outer}}^\ddagger(E, J) \times N_2^\ddagger(E, J)}{N_{\text{outer}}^\ddagger(E, J) + N_1^\ddagger(E, J) + N_2^\ddagger(E, J)}$$

where $N_1^\ddagger(E, J)$ and $N_2^\ddagger(E, J)$ are the E and J resolved number of states for the inner transition state on the terminal and the central carbon atoms, respectively, and $N_{\text{outer}}^\ddagger$ is the number of states of the outer transition state. These formulas are based on a two-transition-state model at the E and J resolved level and assume steady state concentration for the van der Waals complex as well as a collisionless environment between the reactants and the inner transition state.

Although it is possible that the allylic H-abstraction channel has also a low¹⁵ or even submerged¹⁷ energy barrier, it is still significantly higher than that of the addition channels. Therefore, in this work the transition states related to direct H-abstraction are treated as simple tight transition states (i.e. with rigid rotor harmonic oscillator estimates).

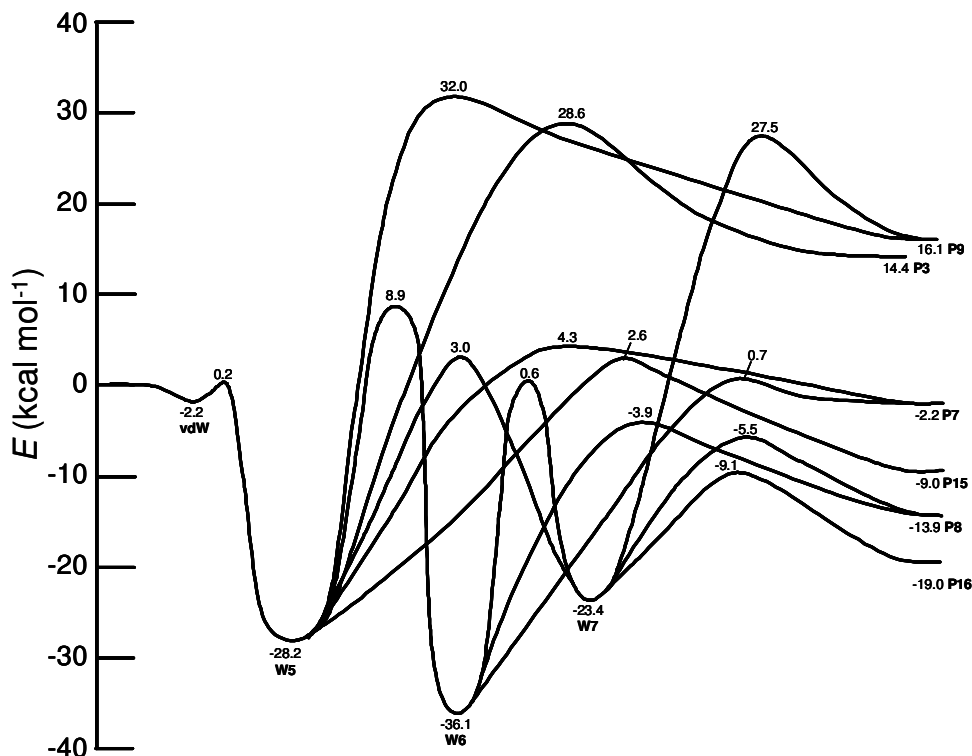


Figure 2. PES for the addition on the central carbon atom. The calculated stationary point energies are obtained by RQCISD(T)/cc-pV ∞ Z//B3LYP/6-311++G(d,p) (except for **W6**↔**P7**) and include the ZPE. The names of the species can be found in Table 1. The height of the inner transition state **vdW**↔**W5** is lowered to -2.3 kcal mol $^{-1}$ in the rate coefficient calculations (see text).

Results and Discussion

The C₃H₇O PES

Addition of the OH radical can take place on the terminal (Fig. 1) carbon atom, forming 1-hydroxy-prop-2-yl (**W1**) or on the secondary carbon (Fig. 2) forming 2-hydroxy-prop-1-yl (**W5**). These complexes are collisionally stabilized and/or undergo isomerization and dissociation leading to various bimolecular products (**P1-P9** and **P14-P17**). The OH radical can also abstract a H-atom directly (Fig 3) forming water and an open shell species (**P10-P13**).

Both addition channels proceed *via* a common van der Waals well, **vdW**. The structure of **vdW** is very similar to that in the C₂H₄ + OH system: the OH bond is approximately perpendicular to the plane of the propene and the H atom is pointing towards the middle point of the C-C double bond. The paper of Szóri et al.¹⁵ confirmed that the abstraction of the allylic H also proceeds *via* the same complex and they did not find any other van der Waals complexes of propene and OH. The abstraction of the other hydrogen atoms is very likely to proceed also through the same complex.

The inner transition states **vdW**↔**W1** and **vdW**↔**W5** were not found using the B3LYP density functional method. Systematic scanning of the B3LYP surface has shown that there is no maximum on the

surface, except for a very small one (<0.2 kcal mol $^{-1}$) at ~ 3 Å, which does not correspond to the transition state sought. Using other quantum chemical methods we are able to locate the geometries of the inner transition state and in this work we are using the ones obtained by second order Møller-Plesset perturbation theory, MP2 with the 6-311++G(d,p) basis set. We also located these structures using CASPT2(3e,3o)/cc-pVDZ and QCISD/6-311++G(d,p) levels of theory. The three geometries are slightly different, e.g. in the MP2 structure the OH is somewhat (~ 0.1 Å) closer to the

Table 1. Species corresponding to the notations on Figs. 1-3.

	species		species
W1	CH ₃ C*HCH ₂ OH	P6	oxetane + H
W2	CH ₃ CH ₂ C*HOH	P7	propen-2-ol + H
W3	CH ₃ CH ₂ CH ₂ O*	P8	acetone + H
W4	C*H ₂ CH ₂ CH ₂ OH	P9	epoxypropane + H
W5	CH ₃ CH(OH)C*H ₂	P10	cis-propen-1-yl + H ₂ O
W6	CH ₃ C*(OH)CH ₃	P11	trans-propen-1-yl + H ₂ O
W7	CH ₃ CH(O*)CH ₃	P12	propen-2-yl + H ₂ O
P1	cis-1-propenol + H	P13	allyl radical + H ₂ O
P2	trans-1-propenol + H	P14	ethene + CH ₂ OH
P3	cyclopropanol + H	P15	vinyl alcohol + CH ₃
P4	propanal + H	P16	acetaldehyde + CH ₃
P5	ethyl + CH ₂ O	P17	allyl alcohol + H

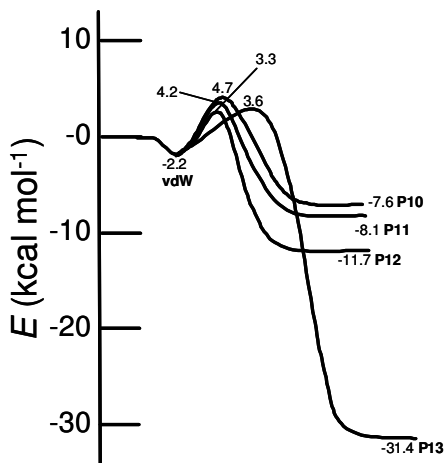


Figure 3. PES for the abstraction channels. The calculated stationary point energies are obtained by RQCISD(T)/cc-pV ∞ Z//B3LYP/6-311++G(d,p) (for the exceptions see text) and include the ZPE. The names of the species can be found in Table 1.

double bond. However, it is expected that applying a high level energy calculation on these different geometries will lead to very similar energies.³³ The energies shown in Figs. 1 and 2 for these saddle points (0.2 kcal mol⁻¹) were obtained at the RQCISD(T)/cc-pV ∞ Z//MP2/6-31++G(d,p) level of theory.

When the OH adds to the terminal C-atom, the most probable bimolecular products are cis- and trans-1-propenol + H (**P1** and **P2**), propanal + H (**P4**) and ethyl + CH₂O (**P5**). Although the exit channels leading to ethene + CH₂OH (**P14**) and vinyl alcohol + CH₃ (**P15**) are also low, the preceding isomerization steps have relatively high barriers, therefore low yields of these products are expected. However, **P15** can also be formed by addition to the central carbon atom, and there is no isomerization step involved. Note that the transition structure **W6** \leftrightarrow **P7** could be located only when using MP2/6-311++G(d,p).

The lowest energy channel in the terminal addition case leads to the formation of acetaldehyde and a methyl group (**P16**). The other low-energy channels lead to the formation of acetone + H (**P8**) and vinyl alcohol + CH₃ (**P15**).

The direct H-abstraction channels can lead to cis- and trans-propen-1-yl (**P10** and **P11**), propen-2-yl (**P12**) and allyl radical (**P13**), always with a H₂O molecule. The barriers leading to these products are significantly higher than the entrance channel. Szőri et al.¹⁵ found two transition states for the allylic abstraction, which we found to be rotamers of each other (also suggested by the authors) separated by a second-order saddle point. Note also that the allylic transition state was found by MP2/6-311++G(d,p) but not by B3LYP/6-311++G(d,p). In the extensive study of Szőri et al.¹⁵ the barrier for the allylic abstraction was found to be lower compared to ours, +0.74 kcal mol⁻¹.

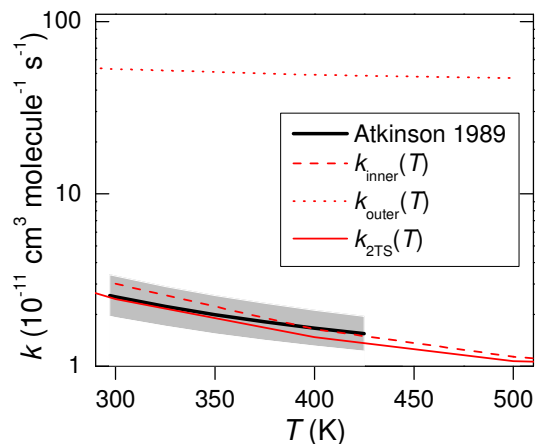


Figure 4. The calculated high pressure limit rate coefficients and its relation to the data evaluation of Atkinson.¹ They gray stripe is the evaluated two least-squares standard deviations of the experimental data. The rate coefficients obtained by using the outer or the inner transition states only are also shown.

The Q1 diagnostic of Lee et al.^{34, 35} indicates the multireference character of the wave function. For most of our stationary points the value of Q1 is small (<0.02), meaning that using a single-reference method is appropriate. For the transition states **vdW** \leftrightarrow **W1**, **vdW** \leftrightarrow **W5**, **vdW** \leftrightarrow **P10-P13** the diagnostic is higher (0.026-0.028) indicating higher uncertainty in these QCISD(T) energies.

The temperature and pressure dependence of the kinetics between 300 K and 500 K

In this temperature region, addition dominates over abstraction. Fig. 4 shows our calculated high-pressure limit rate constant for 300-500 K along with the data evaluation of Atkinson,¹ which is based on numerous experimental results. This figure also shows the capture rate assuming that either only the inner or only the outer transition states are present in the addition channel.

Using our calculated barrier height of +0.2 kcal mol⁻¹ for both entrance channels the rate of addition is low by a factor of ~10 compared to the experiments. In order to get an agreement at 300 K both transition state energies are lowered to -2.3 kcal mol⁻¹. This accords with the C₂H₄ + OH case, although the TS energy in that case had to be lowered by 1 kcal mol⁻¹ only, relative to the high-level *ab initio* value. In the paper of Alvarez-Idaboy et al.¹⁷ the predicted barrier height is -2.1 kcal mol⁻¹ using PMP4/6-311+G(d,p)//MP2/6-311G(d,p) theoretical model chemistry. One possible reason for this relatively big discrepancy is the fact that the PES is extremely shallow in directions perpendicular to the reaction coordinate. Due to the uncertainties in the calculated barrier heights and in the absence of experimental evidence we are not

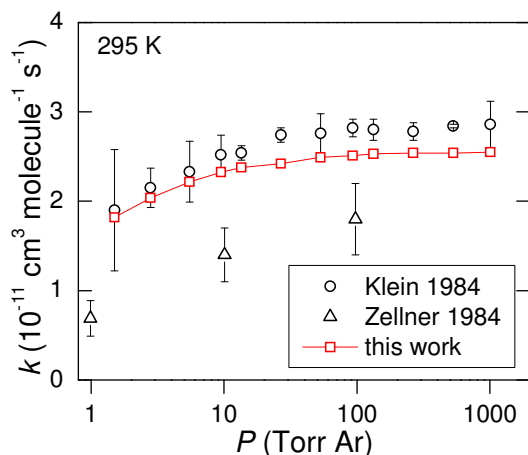


Figure 5. Pressure dependence of the $C_3H_6 + OH$ reaction at 295 K. Error bars are 2σ experimental uncertainties.

in the position to change the two barrier heights independently from each other.

At 300 K the outer transition state lowers the calculated overall rate coefficient by approx 20%, from $3.0 \times 10^{-11} \text{ cm}^3 \text{ molecule}^{-1} \text{ s}^{-1}$ to $2.5 \text{ cm}^3 \text{ molecule}^{-1} \text{ s}^{-1}$ and this effect vanishes at higher temperatures. The contribution of the inner and the outer transition states become equal at ~ 100 K. We obtained a good agreement with the experiment for the temperature dependence in this region.

In Fig. 5 the experimental and the calculated pressure dependent rate coefficients are compared at 295 K in Ar diluent. Klein et al.¹⁰ observed a $\sim 30\%$ decrease in the rate coefficient from 1000 Torr to 1.5 Torr; the decrease in the rate coefficient for Zellner et al.¹¹ is greater. Our model predicts a fall-off behavior very similar to that of Klein et al.¹⁰ The rate coefficient under collisionless conditions is $\sim 8 \times 10^{-15} \text{ cm}^3 \text{ molecule}^{-1} \text{ s}^{-1}$ at 295 K.

The kinetics of the $C_3H_6 + OH$ reaction above 700 K

In this temperature region the reaction is expected to proceed *via* H-abstraction as well as *via* addition followed by rearrangement and dissociation. The latter is likely due to the low-lying barriers. The abstraction reaction has no pressure dependence, while the formation of the other bimolecular products is influenced by both pressure and temperature.

In Fig. 6 the H-abstraction channels are shown along with the data evaluation estimates of Tsang². The calculated rate coefficients generally agree well with the experimental values, although our calculated allylic hydrogen abstraction rate coefficient is outside the uncertainty limits below 800 K.

The bimolecular channels other than abstraction play only a minor role at these temperatures. The overall rate coefficient of their formation at 1 atm between 700 and 1200 K is the same as the rate coefficient for the non-allylic H-atom abstraction. The main (other)

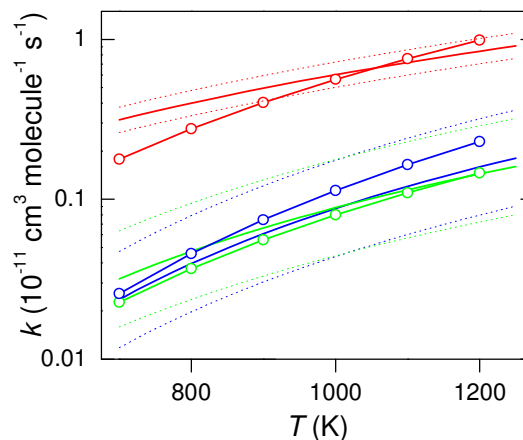


Figure 6. Calculated and evaluated rate coefficients at high temperature. Red: allyl radical + H_2O (**P13**); blue: cis-propen-1-yl + H_2O and trans-propen-1-yl + H_2O (**P10+P11**); green: propen-2-yl + H_2O (**P12**). Lines are the recommendations of Tsang² (uncertainty limits are also shown), the lines with symbols are the calculated values.

bimolecular products at 1 atm are cis-1-propenol + H (**P1**), trans-1-propenol + H (**P2**), propen-2-ol + H (**P7**), vinyl alcohol + CH_3 (**P15**), acetaldehyde + CH_3 (**P16**) and allyl alcohol + H (**P17**).

Conclusions

In this paper we presented parts of our theoretical results for the propene + OH reaction in a wide temperature and pressure range. Our results are in accordance with the experimental data found in the literature; we were able to reproduce both the temperature and pressure dependence of the reaction. Our model can be thus used to answer specific questions regarding product distribution and overall rate coefficients required for combustion modeling.

Acknowledgements

The authors thank Yuri Georgievskii for providing the VaReCoF code for the VRC-TST calculations. This work is supported by the Division of Chemical Sciences, Geosciences, and Biosciences, the Office of Basic Energy Sciences, the U. S. Department of Energy. Sandia is a multi-program laboratory operated by Sandia Corporation, a Lockheed Martin Company, for the National Nuclear Security Administration under contract DE-AC04-94-AL85000.

References

- [1] R. Atkinson, *J. Phys. Chem. Ref. Data* 1 (1989).
- [2] W. Tsang, *J. Phys. Chem. Ref. Data* 20 (1991) 221-273.
- [3] M. Kamphus, B.-U. Marina, K. Kohse-Höinghaus, *Proc. Combust. Inst.* 152 (2008) 28-59.

- [4] C.J. Pope, J.A. Miller, *Proc. Combust. Inst.* 28 (2000) 1519-1527.
- [5] K. Hoyer mann, F. Mauss, T. Zeuch, *Phys. Chem. Chem. Phys.* 6 (2004) 3824-3835.
- [6] H. Böhm, A. Lamprecht, B. Atakan, K. Kohse-Höinghaus, *Phys. Chem. Chem. Phys.* 2 (2000) 4956-4961.
- [7] T. Spangenberg, S. Kohler, B. Hansmann, U. Wachsmuth, B. Abel, M.A. Smith, *J. Phys. Chem. A* 108 (2004) 7527-7534.
- [8] F.P. Tully, J.E.M. Goldsmith, *Chem. Phys. Lett.* 116 (1985) 345-352.
- [9] J.F. Bott, N. Cohen, *Int. J. Chem. Kinet.* 23 (1991) 1075-1094.
- [10] T. Klein, I. Barnes, K.H. Becker, E.H. Fink, F. Zabel, *J. Phys. Chem.* 88 (1984) 5020-5025.
- [11] R. Zellner, K. Lorenz, *J. Phys. Chem.* 88 (1984) 984-989.
- [12] K. Hoyer mann, R. Sievert, *Ber. Bunsen-Ges. Phys. Chem.* 83 (1979) 933-939.
- [13] W.P. Hess, F.P. Tully, *Chem. Phys. Lett.* 152 (1989) 183-189.
- [14] J.R. Dunlop, F.P. Tully, *J. Phys. Chem.* 97 (1993) 6457-6464.
- [15] M. Szöri, C. Fittschen, I.G. Csizmadia, B. Viskolcz, *J. Chem. Theor. Comp.* 2 (2006) 1575-1586.
- [16] I. Diaz-Acosta, J.R. Alvarez-Idaboy, A. Vivier-Bunge, *Int. J. Chem. Kinet.* 31 (1999) 29-36.
- [17] J.R. Alvarez-Idaboy, I. Diaz-Acosta, A. Vivier-Bunge, *J. Comput. Chem.* 19 (1998) 811-819.
- [18] A.M. El-Nahas, T. Uchimaru, M. Sugie, K. Tokuhashi, A. Sekiya, *J. Molec. Struct. - Theochem* 770 (2006) 59-65.
- [19] J.M.L. Martin, *Chem. Phys. Lett.* 259 (1996) 669-678.
- [20] M.J. Frisch, G.W. Trucks, H.B. Schlegel, G.E. Scuseria, M.A. Robb, J.R. Cheeseman, J. Montgomery, J. A., T. Vreven, K.N. Kudin, J.C. Burant, J.M. Millam, S.S. Iyengar, J. Tomasi, V. Barone, B. Mennucci, M. Cossi, G. Scalmani, N. Rega, G.A. Petersson, H. Nakatsuji, M. Hada, M. Ehara, K. Toyota, R. Fukuda, J. Hasegawa, M. Ishida, T. Nakajima, Y. Honda, O. Kitao, H. Nakai, M. Klene, X. Li, J.E. Knox, H.P. Hratchian, J.B. Cross, V. Bakken, C. Adamo, J. Jaramillo, R. Gomperts, R.E. Stratmann, O. Yazyev, A.J. Austin, R. Cammi, C. Pomelli, J.W. Ochterski, P.Y. Ayala, K. Morokuma, G.A. Voth, P. Salvador, J.J. Dannenberg, V.G. Zakrzewski, S. Dapprich, A.D. Daniels, M.C. Strain, O. Farkas, D.K. Malick, A.D. Rabuck, K. Raghavachari, J.B. Foresman, J.V. Ortiz, Q. Cui, A.G. Baboul, S. Clifford, J. Cioslowski, B.B. Stefanov, G. Liu, A. Liashenko, P. Piskorz, I. Komaromi, R.L. Martin, D.J. Fox, T. Keith, M.A. Al-Laham, C.Y. Peng, A. Nanayakkara, M. Challacombe, P.M.W. Gill, B. Johnson, W. Chen, M.W. Wong, C. Gonzalez, J.A. Pople *Gaussian 03*, Revision C.02; Gaussian, Inc.: Wallingford, CT, 2004.
- [21] H.-J. Werner, P.J. Knowles, R. Lindh, F.R. Manby, M. Schütz, P. Celani, T. Korona, G. Rauhut, R.D. Amos, A. Bernhardsson, A. Berning, D.L. Cooper, M.J.O. Deegan, A.J. Dobbyn, F. Eckert, C. Hampel, G. Hetzer, A.W. Lloyd, S.J. McNicholas, W. Meyer, M.E. Mura, A. Nicklass, P. Palmieri, R. Pitzer, U. Schumann, H. Stoll, A.J. Stone, R. Tarroni, T. Thorsteinsson *MOLPRO, a package of ab initio programs* version 2006.1; 2006.
- [22] S.J. Klippenstein, J.A. Miller, *J. Phys. Chem. A* 106 (2002) 9267-9277.
- [23] J.A. Miller, S.J. Klippenstein, *J. Phys. Chem. A* 107 (2003) 2680-2692.
- [24] J.A. Miller, S.J. Klippenstein, *J. Phys. Chem. A* 110 (2006) 10528-10544.
- [25] K.S. Pitzer, W.D. Gwinn, *J. Chem. Phys.* 10 (1942) 428-440.
- [26] M.J. Assael, T.F. Tsolakis, J.P.M. Trusler, *Thermophysical Properties of Fluids : An Introduction to Their Prediction* Imperial College Press London, 1996.
- [27] S.J. Klippenstein, A.F. Wagner, R.C. Dunbar, D.M. Wardlaw, S.H. Robertson, J.A. Miller *VARIFLEX*, 2.0m; 2008.
- [28] Y. Georgievskii, S.J. Klippenstein, *J. Chem. Phys.* 118 (2003) 5442-5455.
- [29] Y. Georgievskii, S.J. Klippenstein, *J. Phys. Chem. A* 107 (2003) 9776-9781.
- [30] J.P. Senosiain, S.J. Klippenstein, J.A. Miller, *J. Phys. Chem. A* 110 (2006) 6960-6970.
- [31] E.E. Greenwald, S.W. North, Y. Georgievskii, S.J. Klippenstein, *J. Phys. Chem. A* 109 (2005) 6031-6044.
- [32] Y. Georgievskii, S.J. Klippenstein *VaReCoF*, Sandia National Laboratories and Argonne National Laboratory: 2006.
- [33] L.B. Harding, S.J. Klippenstein, A.W. Jasper, *Phys. Chem. Chem. Phys.* 9 (2007) 4055-4070.
- [34] T.J. Lee, A.P. Rendell, P.R. Taylor, *J. Phys. Chem.* 94 (1990) 5463-5468.
- [35] T.J. Lee, P.R. Taylor, *Int. J. Quant. Chem.* Supplement 23 (1989) 199-207.